

Competition between the Charge Transfer State and the Singlet States of Donor or Acceptor Limiting the Efficiency in Polymer:Fullerene Solar Cells

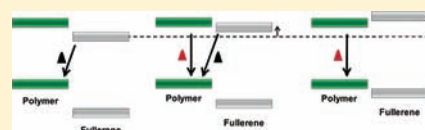
Mark A. Faist,^{†,‡} Thomas Kirchartz,[†] Wei Gong,^{†,§} Raja Shahid Ashraf,[‡] Iain McCulloch,[‡] John C. de Mello,[‡] Nicholas J. Ekins-Daukes,[†] Donal D. C. Bradley,[†] and Jenny Nelson^{*,†}

[†]Department of Physics and Centre of Plastic Electronics, [‡]Department of Chemistry and Centre of Plastic Electronics Imperial College London, South Kensington SW7 2AZ, United Kingdom

[§]Key Laboratory of Luminescence and Optical Information, Ministry of Education and Institute of Optoelectronics Technology, Beijing Jiaotong University, Beijing 100044, People's Republic of China

S Supporting Information

ABSTRACT: We study the appearance and energy of the charge transfer (CT) state using measurements of electroluminescence (EL) and photoluminescence (PL) in blend films of high-performance polymers with fullerene acceptors. EL spectroscopy provides a direct probe of the energy of the interfacial states without the need to rely on the LUMO and HOMO energies as estimated in pristine materials. For each polymer, we use different fullerenes with varying LUMO levels as electron acceptors, in order to vary the energy of the CT state relative to the blend with [6,6]-phenyl C61-butyric acid methyl ester (PCBM). As the energy of the CT state emission approaches the absorption onset of the blend component with the smaller optical bandgap, $E_{\text{opt,min}} \equiv \min\{E_{\text{opt,donor}}; E_{\text{opt,acceptor}}\}$, we observe a transition in the EL spectrum from CT emission to singlet emission from the component with the smaller bandgap. The appearance of component singlet emission coincides with reduced photocurrent and fill factor. We conclude that the open circuit voltage V_{OC} is limited by the smaller bandgap of the two blend components. From the losses of the studied materials, we derive an empirical limit for the open circuit voltage: $V_{\text{OC}} \lesssim E_{\text{opt,min}}/e - (0.66 \pm 0.08)\text{eV}$.



1. INTRODUCTION

Solar cells made from solution processable materials such as polymer:fullerene bulk heterojunctions have the potential to substantially reduce the cost of solar energy conversion, provided their power conversion efficiency can be further optimized. In order to maximize the power conversion efficiency of solar cells for a given optical bandgap E_{opt} it is essential to convert a high number of absorbed photons into collected charge carriers and to maximize the free energy per extracted charge carrier, i.e. the voltage. The maximum free energy per photogenerated charge carrier corresponds to the open circuit voltage. The difference between eV_{OC} measured as one sun equivalent light intensity and the optical bandgap E_{opt} $\Delta E = E_{\text{opt}} - eV_{\text{OC}}$ is therefore a conventional way to quantify the energy loss of a solar cell.^{1,2} In organic solar cells, ΔE is typically between 0.8 and 1.3 eV,^{3–7} much larger than the difference between band gap and V_{OC} in crystalline silicon solar cells^{8,9} of around 0.4–0.5 eV.¹⁰

While in inorganic solar cells an absorbed photon directly creates a pair of free carriers, in organic solar cells an absorbed photon results in a tightly bound exciton due to the low dielectric constant of the organic absorber materials.^{11,12} To separate this exciton into free charge carriers, a type II heterojunction between an electron-accepting and an electron-donating material is required. The energy offset at the type II heterojunction allows efficient charge separation¹³ but introduces an additional energy loss. After exciton separation,

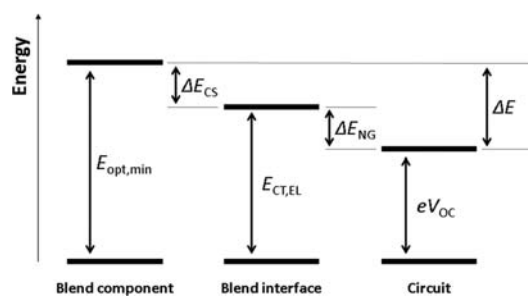
the charge carriers form a charge transfer state with an energy E_{CT} . Different definitions for the energy E_{CT} exist,^{14–16} but all are related to the energy of the free charge carriers, the electron residing on the lowest unoccupied molecular orbital (LUMO) of the acceptor and the hole residing on the highest occupied molecular orbital (HOMO) of the donor. Scheme 1 depicts the different energy levels involved, namely the minimum of the absorption onset of donor and acceptor $E_{\text{opt,min}} \equiv \min\{E_{\text{opt,donor}}; E_{\text{opt,acceptor}}\}$, the CT state as well as eV_{OC} , the free energy of an electron at the cathode at open circuit voltage. As a definition for the CT state we employ the definition used by Tvingstedt et al., which relates the CT state to its electroluminescence emission peak.¹⁷ This emission originates from a charge transfer exciton formed by free charge carriers that have previously been injected from the electrodes. For simplicity, we will refer to this emission simply as CT emission.

The definition of $E_{\text{CT,EL}}$ allows us to divide the loss $\Delta E = E_{\text{opt}} - eV_{\text{OC}}$ between absorption onset E_{opt} and open circuit voltage V_{OC} into two quantifiable contributions ΔE_{CS} and ΔE_{NG} : $\Delta E_{\text{CS}} = E_{\text{opt}} - E_{\text{CT,EL}}$, a loss related to the energy offset required for exciton separation, and $\Delta E_{\text{NG}} = E_{\text{CT,EL}} - eV_{\text{OC}}$, a loss linked to nongeminate recombination.^{18–20}

Minimizing ΔE_{CS} by raising the energy of the CT state while still enabling efficient charge separation is consequently one of

Received: October 25, 2011

Published: November 29, 2011

Scheme 1. Energetic Losses in a Type II Heterojunction Organic Solar Cell^a

^a ΔE_{CS} is the loss between the smaller absorption onset of the two blend components $E_{opt,min}$ and the peak of the CT state electroluminescence $E_{CT,EL}$; ΔE_{NG} is the loss between $E_{CT,EL}$ and the free energy of an electron at open circuit voltage eV_{OC} ; ΔE is the total energy loss.

the main design strategies for new donor and acceptor materials.²¹ Several studies have shown that if the CT state energy is raised above a certain threshold, it competes with other neutral excited states.^{22,23} Westenhoff et al. studied polymer:polymer blends with high open circuit voltages and suggested triplet excitons as loss pathway limiting generation of separated charges.²⁴ Fullerene triplet excitons were detected in polymer:fullerene blends with high CT state energies, but it remained unclear whether these were formed by energy transfer from the CT state or populated from the fullerene singlet.^{25,26}

One of the main restrictions of these and other studies^{3,15,27–29} is, however, the difficulty of measuring an absolute value for E_{CT} . Usually it is estimated from energy levels of the pristine materials which are subject to large uncertainties. A famous example is the lowest unoccupied molecular orbital (LUMO) of [6,6]-phenyl C61-butyric acid methyl ester (PCBM), the typically used acceptor material in organic solar cells. The reported LUMO values vary between -3.7 eV and -4.3 eV.^{15,30–32} Even if the determination of energy levels is done with one consistent method in pristine materials, the results may not be transferable to blend films and devices, because effects such as aggregation, crystallization, and interface dipoles can shift energy levels by up to 0.5 eV.^{33–37} These uncertainties in energy levels are relevant for material design rules and for the estimation of efficiency potentials as done by Scharber et al.¹⁵

The present contribution uses electroluminescence (EL) and photoluminescence (PL) measurements of polymer:fullerene devices and films to study the relationship between interfacial energetics and charge generation and recombination. EL spectroscopy probes the emissive states directly in working devices and allows a quantitative determination of the energy of the CT state by measuring its emission.¹⁷ We alter the energy of the CT state by combining a series of polymers with different fullerenes featuring a 400 meV range of LUMO energies, using PCBM and indenofullerenes with one (ICMA), two (ICBA), or three (ICTA) adducts as acceptors. This allows us to explore the effect of reduced ΔE_{CS} on photocurrent generation and electroluminescence emission. We observe that, if the energy of the CT state approaches the smaller absorption onset of the two blend components, $E_{opt,min}$, activation of the component singlet occurs. This appearance of singlet emission coincides with a reduction in photocurrent and therefore poor device

performance. This allows us to derive an empirical limit for CT state energy and V_{OC} relative to $E_{opt,min}$.

2. EXPERIMENTAL DETAILS

Poly(3-hexylthiophene) (P3HT) was purchased from Merck, Poly((4,4'-bis(2-ethylhexyl)dithieno[3,2-*b*:2',3'-*d*]silole)-2,6-diyl-alt-(4,7-bis(2-thienyl)-2,1,3-benzothiadiazole)-5,5'-diyl) (SiPCPDTBT) was received from Konarka, Poly(2-methoxy-5-(3'-7'-dimethyloctyloxy)-1,4-phenylenevinylene (MDMOPPV) from Sigma-Aldrich, and 60PCBM from Nano-C. The indenofullerenes (ICMA, ICBA, ICTA) were received from Plextronics. Poly((9,9-dioctylfluorenyl-2,7-diyl)-alt-5,5-(40,70-di-2-thienyl-20,10,30-benzothiadiazole)) (PFODTBT) was synthesized as described in the Supporting Information.

Bulk heterojunction (BHJ) solar cells were prepared by cleaning patterned ITO in detergent, acetone, and isopropanol. A layer of PEDOT:PSS was spin coated onto the ITO substrates at 2000 rpm and annealed at 150 °C for 20 min. Subsequently, the active layer solution was spin coated on top (P3HT:fullerene (dissolved in chlorobenzene (CB) at 1:1 wt %, 40 mg/mL), MDMO-PPV:fullerene (CB, 1:4 wt %, 25 mg/mL), SiPCPDTBT (dissolved in *o*-dichlorobenzene (ODCB), 1:2 wt %, 40 mg/mL), PFODTBT (ODCB, 1:4 wt %, 30 mg/mL)). Vacuum-deposited aluminum (MDMOPPV:PCBM, PFODTBT:PCBM) or calcium/aluminum (P3HT:PCBM, SiPCPDTBT:PCBM) was used as cathode. All the devices were encapsulated in a nitrogen-filled glovebox.

Differential pulse voltammetry (DPV) was performed as reported before,³⁸ using a 0.1 mM solution of the fullerenes in acetonitrile with TBABF₆ as electrolyte. Electron affinities were measured against ferrocene as internal standard, using platinum as working and counter electrodes and Ag/AgCl as reference electrode.

Electroluminescence (EL) was measured using a Princeton Instruments Acton SP 2500 spectrograph combined with a liquid nitrogen-cooled InGaAs photodiode array (Acton OMAV:1024). Spectral intensity was corrected with the spectrum from a calibrated halogen lamp. All blends shown here are measured at comparable forward current (blends with SiPCPDTBT, MDMOPPV, and P3HT at 200 mA/cm², blends with PFODTBT at 400 mA/cm²). Compared to lower currents, peaks change very little in shape or position (see Supporting Information). The peak position is calculated by integrating the peak and by defining the peak position as the point where the integral is half its maximum.

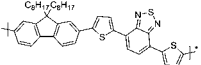
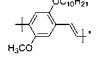
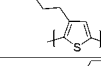
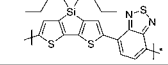
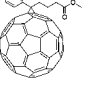
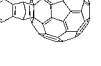
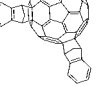
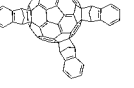
Photoluminescence (PL) was measured with the same detector system using a 473 -nm diode laser as excitation source and corrected for the absorption at the excitation wavelength measured using a Shimadzu UV-2550 spectrometer.

3. RESULTS

To explore the effect of reduced band offsets at the heterojunction on the generation of charges, we investigated blends that show a high open circuit voltage first. Copolymers of fluorene with thienyl benzothiadiazole such as PFODBT lead to the highest reported V_{OC} values (1.0 V) among polymer:PCBM solar cells with a power conversion efficiency (PCE) larger than 4% .^{39–41} The analysis by Vandewal et al. suggests that V_{OC} and energy of the CT state are correlated;^{16,42} thus, for these materials we expect V_{OC} and CT state energy to be close to the highest possible values that are still compatible with efficient charge separation. To explore these limits, we studied blends of PFODTBT with ICMA and ICBA, fullerenes that have a higher-lying LUMO level than that of PCBM (Table 1) and that have been shown to increase V_{OC} in blends with P3HT,⁴³ the most-studied organic photovoltaic material.^{44–47}

Figure 1a shows the electroluminescence from PFODTBT blends with PCBM, ICMA, and ICBA (1:4). The blend with PCBM shows a red-shifted emission compared to both blend

Table 1. Donor Polymers (top) and Acceptor Molecules (bottom) Used in This Study^a

Donor polymer	Molecular structure	V_{oc} in BHJ with PCBM	HOMO level [eV] reported	$E_{CT,EL}$ (with PCBM)
PFODTBT		0.99 ± 0.03	-5.8^4	1.32 ± 0.05
MDMO-PPV		0.85 ± 0.02	-5.3^{48}	1.19 ± 0.03
P3HT		0.58 ± 0.02	-4.6^{36} -5.0^{49}	0.89 ± 0.03
Si-PCPDTBT		0.60 ± 0.02	-5.0^{50}	0.97 ± 0.02
Acceptor molecule	Molecular structure	LUMO level [eV] reported	LUMO level [eV] measured*	
PCBM		-3.7^{30} -4.3^{15} -3.91^{43}	-3.74 ± 0.02	
ICMA		-3.86^{43}	-3.70 ± 0.02	
ICBA**		-3.72^{43}	-3.55 ± 0.02	
ICTA**			-3.36 ± 0.05	

^a* = measured in solution by DPV; ** = fullerene multiadducts are a mixture of different isomers, only one isomer is shown.

components which most likely originates from the CT state.¹⁷ We find the peak center of this emission at $1.32 \text{ eV} \pm 0.05 \text{ eV}$, around 0.33 eV above eV_{OC} .

If we now replace PCBM by ICMA, a fullerene with slightly higher LUMO level, we observe a change in the peak shape that we ascribe to a contribution from the fullerene single which is also shown in Figure 1.

In the case of the PFODTBT:ICBA blend, emission from the fullerene is dominant, and no emission from the CT state is visible. The spectrum remains unchanged in a 4:1 mixture of the PFODTBT:ICBA blend, making it unlikely that the fullerene emission arises from direct injection of electrons and holes into large fullerene domains in which electrons and holes are injected from the electrodes (see Supporting Information).

These data suggest that the higher we raise the energy of the CT state in the blend, the more likely it is that the injected charges are activated into the fullerene and recombine via the fullerene singlet. Photoluminescence data (Figure 1b), corrected for the number of absorbed photons, shows a similar trend. In the blend of PFODTBT with PCBM, the photoluminescence from PFODTBT is strongly quenched (>99%) compared to the pristine film, while a weak red-shifted emission is observed, composed of PCBM singlet emission and CT state luminescence. Emission from the blend with ICBA, however, is

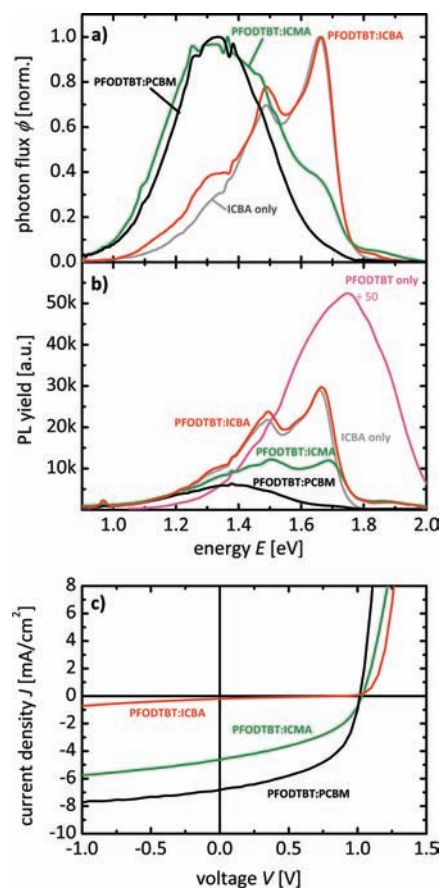


Figure 1. (a) Electroluminescence (EL) of devices with PFODTBT blended with PCBM (black), ICMA (green), and ICBA (red) as active layer. EL of a device with only ICBA as active layer is shown for comparison (gray). The small peak at 1.37 eV is a measurement artifact. (b) Photoluminescence of polymer blends and an ICBA film, corrected for the incoming photons at excitation wavelength (473 nm). (c) Current–voltage curves of devices with blends of PFODTBT with PCBM, ICMA, and ICBA (1:4), measured at approximately 1 sun illumination.

similar in relative and absolute terms to the emission of the pristine ICBA film, even though, at the used excitation wavelength, around 50% of the photons are absorbed by the polymer. This implies that excitons absorbed by the polymer are transferred to the fullerene, where they decay and do not separate into free carriers. The photocurrent (Figure 1c) is greatly reduced for the blend with ICBA as compared to photocurrents for the blends of PFODTBT with PCBM and ICMA. PFODTBT:ICMA shows some PL emission from the fullerene as well, but this could equally originate from micrometer-sized fullerene domains we observed in microscope images (see Supporting Information). In summary, we see that for PFODTBT blends, a reduction of photocurrent correlates with the strength of fullerene emission visible in EL and PL.

A similar transition in EL emission from CT state to fullerene emission can be observed when the polymers MDMOPP and P3HT are blended with fullerene multi-adducts (Figure 2). In blends of MDMOPP:PCBM, the eV_{OC} and the emission from the CT state are around 0.2 eV lower compared to that for PFODTBT, and the transition to fullerene emission occurs in moving from ICBA to ICTA (Figure 2a). In the CT emission of MDMOPP:ICBA a fullerene shoulder is clearly visible, and the blend with ICTA is dominated by fullerene emission. For

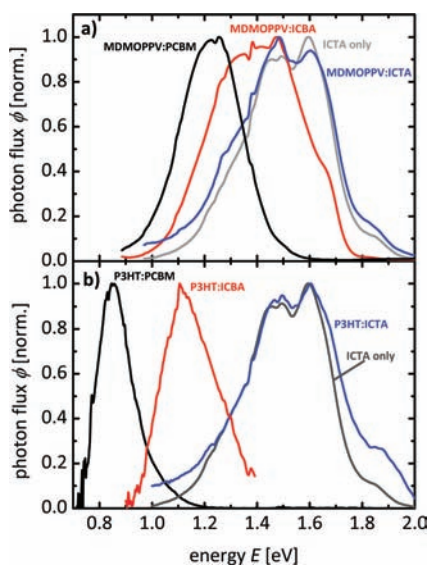


Figure 2. (a) Electroluminescence (EL) of devices with MDMOPPV blended with PCBM (black), ICBA (red), and ICTA (blue) as active layer. EL of a device with pristine ICTA is shown for comparison (gray). The small peak at 1.37 eV is an artifact of the detector. (b) Electroluminescence of blends with P3HT blended with PCBM (black), ICBA (red), and ICTA (blue) as active layer. EL of a device with pristine ICTA is shown for comparison (gray).

P3HT blended with ICBA, $E_{EL,CT}$ is at 1.13 eV, still far below that of the fullerene singlet, and only emission from the charge transfer state is visible. The shape of P3HT:ICTA blend emission, however, strongly resembles the emission from ICTA. Again, the observation of a strong fullerene component in the EL correlates with reduced photocurrent (see Supporting Information). The CT EL quantum yield in blends with P3HT, however, is much lower than the quantum yield of the respective fullerene singlets. This suggests that the emission from the P3HT:ICTA CT state may be masked by the EL emission of the fullerene singlet. This could explain why we see fullerene emission rather than a mixture of fullerene and CT emission.

A clear transition from CT emission to fullerene has been observed in all blends in which the optical bandgap of the fullerene is smaller than the optical bandgap of the polymer. To study the opposite case in which the polymer bandgap is smaller than the fullerene bandgap ($E_{opt,donor} < E_{opt,acceptor}$), we blend the fullerenes with Si-PCPD TBT. This polymer has an absorption onset of around 1.5 eV,⁵⁰ lower than the absorption onset of the fullerene (1.7 eV). Figure 3 shows EL, PL, and device data of SiPCPD TBT and its blends.

It is clearly visible in Figure 3a that in the case of a low polymer bandgap, a transition from CT state to polymer singlet occurs in the EL emission, as opposed to the fullerene singlet emission observed in the previous blends. The blend with ICBA shows a mixture of CT state and polymer singlet emission, while the blend with ICTA is dominated by polymer emission. Once more, a reduction of photocurrent and fill factor is observed with increased singlet emission, this time from the polymer. For the SiPCPD TBT:ICTA blend, the photoluminescence of the polymer is not quenched well (Figure 3b), showing that charge separation or energy transfer from polymer to fullerene is greatly reduced in this blend, owing to the small energy offset between polymer singlet and CT state.

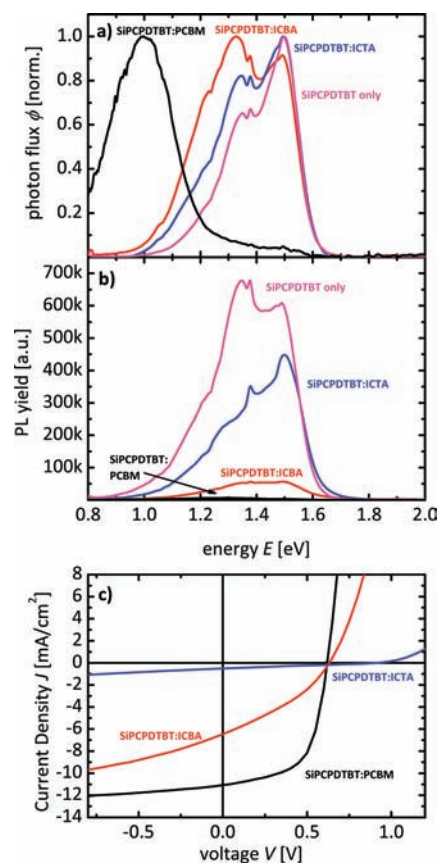


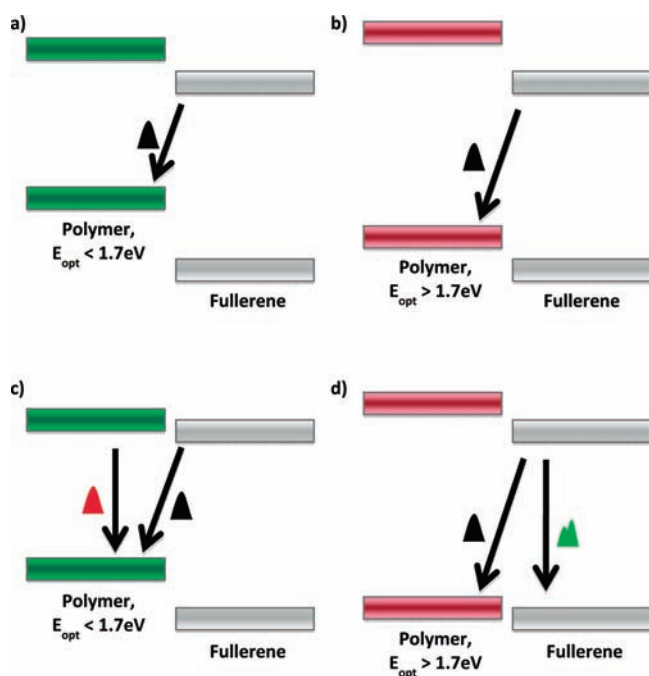
Figure 3. (a) Electroluminescence (EL) of devices with SiPCPD TBT blended with PCBM (black), ICBA (red), and ICTA (blue) as active layer. EL of a device with pristine polymer is shown for comparison (magenta). (b) Photoluminescence (PL) of SiPCPD TBT films blended with PCBM (black), ICBA (red), and ICTA (blue) from an excitation wavelength of 473 nm. The small peak at 1.37 eV is an artifact of the detector. (c) Current–voltage curves of devices with blends of SiPCPD TBT with PCBM, ICBA, and ICTA (1:2), measured at approximately 1 sun illumination.

Despite the fact that at the excitation wavelength of 473 nm around two-thirds of the photons are absorbed by the fullerene, no fullerene emission is detected in any of the blends' PL emissions. This fact, together with extremely small polymer emission observed in PFODTBT:ICBA, shows that energy transfer between the components is considerably faster than singlet exciton decay in polymer and fullerene.

4. DISCUSSION

We found that in all studied blends with PCBM, the EL spectrum is dominated by emission from the charge transfer state with the energy $E_{CT,EL}$ (Scheme 2a,b). As we replace PCBM by fullerene adducts with higher lying LUMO levels, $E_{CT,EL}$ rises similarly to the shift in acceptor LUMO level. As $E_{CT,EL}$ approaches $E_{opt,min}$ (Scheme 2c,d), the observed emission is a composition of CT emission and component singlet emission. Ultimately, for very small $\Delta E_{CS} = E_{opt,min} - E_{CT,EL}$, emission from the lowest-component singlet in the blend dominates. As singlet emission appears in the EL spectra, photoluminescence from the excited singlet is less well quenched and photocurrent is reduced.

We find that electroluminescence to be a powerful tool to study the CT state because of its ability to directly probe the interface states. Photoluminescence generally contains con-

Scheme 2. Electroluminescence in Polymer:Fullerene Blends^a

^a(a,b) The CT state is significantly lower than any component singlet in the blend. EL emission originates from the CT state only. (c,d) As the CT state energy approaches the energy of the lowest singlet of both blend materials, EL emission is a mixture between CT state emission and component singlet emission. The icons next to the arrows represent the peak shapes of the EL emission.

tributions from not separated intramolecular excitons. These contributions are strongly morphology-dependent and overlap with the intermolecular CT emission. In the case of P3HT, the contributions from component excitons even cover the CT emission completely. The EL emission, in contrast, arises from recombination at the polymer:fullerene interface.¹⁷ This implies that singlet states visible in EL must be populated either through energy transfer from the CT state or through charge transfer from one component to the other. It is not possible, however, to distinguish these two different mechanisms within our experiment. Morteani et al. have studied polymer:polymer blends and have shown with temperature-dependent measurements that energy transfer from the CT state dominates below 4 V, with an endothermic activation energy of $200 \text{ meV} \pm 50 \text{ meV}$.^{51–53} Since all of the presented EL spectra have been measured at voltages smaller than 4 V, this would suggest that the principal mechanism is energy transfer from the CT state to a component singlet. The activation energy of 200 meV corresponds to about twice the width of the density of states (DOS) of an organic semiconductor,⁵⁴ which may suggest that singlet emission is linked to an overlap of CT state emission and singlet absorption. Activation might also be facilitated by the increased energetic disorder of fullerene multiadducts⁵⁵ that broaden the DOS and can ease activation.

The activation of the component singlets observed in the EL is relevant for device operation and charge separation. Singlet population from the CT state – regardless whether the mechanism is energy transfer or charge transfer – indicates that the offset at the type II heterojunction is so small that endothermic activation is possible. For such a small offset, the

net rate for charge separation might be significantly reduced, increasing geminate recombination of excitons on the component with lower optical bandgap increased. This is especially relevant for polymer:fullerene blends with $E_{\text{opt,donor}} < 1.70 \text{ eV}$, where – due to the low fullerene absorptivity – most of the current is generated by the component with lower singlet energy. In blends with higher bandgap polymers ($E_{\text{opt,donor}} > 1.70 \text{ eV}$), charge separation could occur directly from the polymer via electron-transfer to the fullerene⁵⁶ and if at short-circuit charge carriers are unlikely to return to the interface, photocurrent may still be high. At open circuit, however, where losses via interfacial recombination are more important, an additional nongeminate recombination pathway through singlet activation is available, reducing fill factor (FF) and open circuit voltage of the solar cell. We have observed this reduction in V_{OC} and FF for all blends with at least partial singlet emission (see Supporting Information), but other factors such as microstructure, transport, or shunts can affect these indicators for device performance as well, so a quantification is not possible in this case.

It is possible, however, to quantify different types of energetic losses using the energy of the CT electroluminescence. We observe a large range of values for ΔE_{CS} in the studied blends, with P3HT:PCBM showing the highest value of 0.81 eV. In PFODTBT:PCBM, the blend with the smallest observed ΔE_{CS} that still produces high photocurrent, the threshold to partial singlet emission occurs at a CT emission peak of around 1.35 eV, about 0.35 eV below the fullerene bandgap of $(1.70 \pm 0.02) \text{ eV}$: $\Delta E_{\text{CS,min}} = (0.35 \pm 0.05) \text{ eV}$. The value of $\Delta E_{\text{CS,min}}$ might differ as a function of the donor polymer, but previous studies indicate that donor block-copolymers with benzothiadiazole (BT) as acceptor unit (as PFODTBT) show charge generation at low energetic offsets.⁵⁷ In all our studied polymers we find that, if ΔE_{CS} falls below 0.35 eV, the blend enters a transition region ($0.35 \ll \Delta E_{\text{CS}} < 0$) in which component singlet activation becomes possible and the net rate for charge separation, fill factor and photocurrent are likely to be reduced. ΔE_{CS} represents the additional energetic loss needed to separate excitons bound by the low dielectric constant of the organic materials, a loss not present in inorganic solar cells. For crystalline silicon (c-Si), for instance, the difference between optical bandgap and peak EL emission is equal to the energy of an optical phonon minus the thermal energy kT , which is around 0.03 eV.^{8,58}

The blend with the smallest observed ΔE_{NG} is P3HT:PCBM with $\Delta E_{\text{NG,min}} = (0.31 \pm 0.03) \text{ eV}$. P3HT is well-known for long lifetimes²⁰ as well as high mobilities in the blend⁵⁹ that have been associated with small losses through nongeminate recombination.²⁰ All of the measured blends show quite similar values for ΔE_{NG} : $0.3 \text{ eV} < \Delta E_{\text{NG}} < 0.4 \text{ eV}$, in agreement with reports by Vandewal et al.¹⁴ Interestingly, these losses are comparable or smaller than the losses between the EL peak (1.09 eV) and the typical eV_{OC} (700 meV) in crystalline silicon solar cells.⁸ To understand the difference between organic bulk heterojunction solar cells and classical crystalline semiconductor solar cells better, it is instructive to split the nongeminate losses further into radiative and nonradiative losses. The reason for the fact that BHJ solar cells have nongeminate losses that are comparable or smaller than those in c-Si is due to the fact that the radiative losses in BHJ solar cells are small compared to the radiative losses in many inorganic solar cells. Thermal emission of a body depends on, according to Kirchhoff's law, the blackbody spectrum and the

absorptance of the body. Luminescent emission of a semiconductor diode follows a similar law and depends on the blackbody spectrum ϕ_{bb} , voltage V , and photovoltaic external quantum efficiency Q_e of the device according to⁶⁰

$$\phi_{\text{EL}} = Q_e \phi_{\text{bb}} \exp\left(\frac{qV}{kT}\right) \quad (1)$$

with k being the Boltzmann constant and T the temperature. This equation holds for pn-junctions with linear recombination rates,⁶¹ i.e. it is an excellent approximation for c-Si and other inorganic materials, but even for organic solar cells there is evidence that this equation provides a decent approximation.^{42,62} According to eq 1, the radiative losses are high when the quantum efficiency at the EL peak is high, i.e. when there is only a small shift between EL peak and absorption onset. This shift is rather massive in bulk heterojunction solar cells, because the quantum efficiency at the CT state is always very low compared to the peak quantum efficiency, while the shift is rather small for inorganic solar cells. The radiative open circuit voltage $V_{\text{oc,rad}}$ is the hypothetical open circuit voltage that a solar cell would have if there was only radiative recombination. This open circuit voltage can be calculated from EL and quantum efficiency measurements as described before^{63,64} using

$$V_{\text{OC,rad}} = \frac{kT}{q} \ln\left(\frac{J_{\text{SC}}}{q \int Q_e \phi_{\text{bb}} dE}\right) \quad (2)$$

with q being the electric charge. The energy $eV_{\text{oc,rad}}$ corresponding to the radiative open circuit voltage, is often close to the EL peak in organic solar cells (e.g., $V_{\text{oc,rad}}(\text{PFODTBT}) = 1.34$ V, $E_{\text{EL,CT}}(\text{PFODTBT}) = 1.32$ eV), while the $eV_{\text{oc,rad}}$ of crystalline semiconductor solar cells is considerably below the band gap (e.g., $V_{\text{oc,rad}}(\text{c-Si}) = 864$ mV, $E_g(\text{c-Si}) = 1.124$ eV).^{63,64} The nonradiative losses in organic solar cells are huge compared to the radiative losses (hence the low luminescence efficiency of the CT state),⁴² but they are small compared to crystalline silicon solar cells, if we compare the difference between the peak of the EL and the V_{oc} . This is probably due to the blend structure that separates electrons from holes and suppresses nongeminate recombination. Further reduction of nongeminate recombination by reducing the concentration of localized states^{65–68} which facilitate recombination is thus an additional promising pathway to higher efficiencies because of its positive effect on both V_{oc} and the fill factor.

Going back to the losses due to charge separation and nongeminate recombination, we can now investigate lower limits for energy losses in organic solar cells. The sum of the two minimal losses, $\Delta E_{\text{CS,min}}$ and $\Delta E_{\text{NG,min}}$, enables us to set an empirical limit for the open circuit voltage of an efficient organic solar cell. The V_{OC} is limited by the smaller optical bandgap of either donor or acceptor minus a minimal energy loss:

$$eV_{\text{OC}} \lesssim \min\{E_{\text{opt,donor}}; E_{\text{opt,acceptor}}\} - \Delta E_{\text{min}} \quad (3)$$

with

$$\begin{aligned} \Delta E_{\text{min}} &= \Delta E_{\text{CS,min}} + \Delta E_{\text{NG,min}} \\ &= 0.35\text{eV} + 0.31\text{eV} \\ &= (0.66 \pm 0.08)\text{eV} \end{aligned} \quad (4)$$

This is in good agreement to a value of 0.6 V reported by Veldman et al.,³ but our study provides substantial insight into the composition of this value.

The V_{OC} limit has implications especially for donors with optical bandgaps higher than the fullerene ($E_g > 1.7$ eV). Their open circuit voltage is limited by the fullerene to around 1 V, while most of the absorption occurs above the polymer bandgap, resulting in an additional energy loss (e.g., 0.2–0.3 eV for P3HT and PFODTBT). This also explains why open-circuit voltages of these polymer:fullerene solar cells have been limited to around 1 V.⁴⁰ Higher open circuit voltages (1.2–1.4 V) have been observed solely in blends containing nonfullerene acceptors with higher optical bandgaps.^{69–72} Different acceptors might therefore be needed in organic tandem solar cells, for which the optimal bandgap may lay above 1.7 eV, depending on the low-bandgap subcell.⁷³

A research of the literature shows that the lowest energy loss reported for single junction polymer:fullerene cells is $\Delta E = 0.69$ eV, realized in a blend composed of a diketopyrrolopyrrole-based copolymer and PC₇₀BM.⁷⁴ It features a relatively high fill factor ($FF = 0.60$) but shows a low external quantum efficiency. The most efficient reported cells, devices with 8.3% power conversion efficiency,^{75,76} operate at an $\Delta E = 0.85$ – 0.90 eV. Assuming $\Delta E_{\text{NG}} \leq 0.4$ eV, this results in a $\Delta E_{\text{CS}} > 0.45$ eV, indicating significant improvement potential by reducing the energetic losses of the solar cells.

5. CONCLUSION

We used EL and PL spectroscopy to study a selection of high-performance polymers blended with a series of fullerenes featuring different LUMO levels. Measurement of the electroluminescence of the charge transfer state allows a determination of the CT state energy directly in the device and is therefore much better suited to study the limits of the CT state than methods based on the measurement of electrochemical energy levels measured in pristine materials. We found that singlet activation in the EL occurs when the difference ΔE_{CS} between the energy of the CT emission, $E_{\text{CT,EL}}$, and the lowest component absorption onset, $E_{\text{opt,min}}$, is smaller than 0.35 eV. This singlet activation is correlated to a reduction in PL quenching and photocurrent generation; for $0 < \Delta E_{\text{CS}} < 0.35$ eV, we observe a transition from a working device with pure CT emission to devices with strongly reduced photocurrent and predominantly polymer or fullerene singlet emission. This allows us to derive an empirical limit for V_{OC} for efficient polymer:fullerene solar cells which is related to the lowest absorption onset of the components in the blend: $V_{\text{OC}} \lesssim E_{\text{g,min}}/e - 0.66$ V

■ ASSOCIATED CONTENT

📄 Supporting Information

Synthesis of PFODTBT, additional electroluminescence spectra of PFODTBT:ICBA (4:1) and pristine fullerenes, normalized photoluminescence spectra, determination of absorption onsets, additional current–voltage curves and device parameters, current-dependent electroluminescence spectra. This material is available free of charge via the Internet at <http://pubs.acs.org>

■ AUTHOR INFORMATION

Corresponding Author

jenny.nelson@imperial.ac.uk

ACKNOWLEDGMENTS

We thank Konarka Technologies for providing SiPCPDTBT, Plextronics Inc., for providing the indenofullerenes, and Darin Laird and Shawn Williams from Plextronics for fruitful discussions. Thanks to Louise Hirst and Markus Fuhrer for their help with the electroluminescence setup. We acknowledge for funding EPSRC (EP/F061757/1) and the Carbon Trust (Applied Research Project No. 064-179). W.G. acknowledges support from P.R. China's State Scholarship Fund. T.K. acknowledges support by an Imperial College Junior Research Fellowship. J.N. thanks the Royal Society for the award of an Industrial Fellowship.

REFERENCES

- (1) Dennler, G.; Scharber, M. C.; Brabec, C. J. *Adv. Mater.* **2009**, *21*, 1323–1338.
- (2) Nayak, P. K.; Bisquert, J.; Cahen, D. *Adv. Mater.* **2011**, *23*, 2870–2876.
- (3) Veldman, D.; Meskers, S. C. J.; Janssen, R. A. J. *Adv. Funct. Mater.* **2009**, *19*, 1939–1948.
- (4) Admassie, S.; Inganäs, O.; Mammo, W.; Perzon, E.; Andersson, M. R. *Synth. Met.* **2006**, *156*, 614–623.
- (5) Blouin, N.; Michaud, A.; Leclerc, M. *Adv. Mater.* **2007**, *19*, 2295–2300.
- (6) Chen, H.-Y.; Hou, J.; Zhang, S.; Liang, Y.; Yang, G.; Yang, Y.; Yu, L.; Wu, Y.; Li, G. *Nat. Photonics* **2009**, *3*, 649–653.
- (7) Mühlbacher, D.; Scharber, M.; Morana, M.; Zhu, Z.; Waller, D.; Gaudiana, R.; Brabec, C. *Adv. Mater.* **2006**, *18*, 2884–2889.
- (8) Kirchartz, T.; Helbig, A.; Reetz, W.; Reuter, M.; Werner, J. H.; Rau, U. *Prog. Photovoltaics: Res. Appl.* **2009**, *17*, 394–402.
- (9) Green, M. A. *Prog. Photovoltaics: Res. Appl.* **2011**, DOI: 10.1002/pip.1147.
- (10) King, R. R.; Bhusari, D.; Boca, A.; Larrabee, D.; Liu, X. -Q.; Hong, W.; Fetzer, C. M.; Law, D. C.; Karam, N. H. *Prog. Photovoltaics: Res. Appl.* **2011**, *19*, 797–812.
- (11) Gregg, B. A. J. *Phys. Chem. B* **2003**, *107*, 4688–4698.
- (12) Blom, P. W. M.; Mihailtchi, V. D.; Koster, L. J. A.; Markov, D. E. *Adv. Mater.* **2007**, *19*, 1551–1566.
- (13) Tang, C. W. *Appl. Phys. Lett.* **1986**, *48*, 183–185.
- (14) Vandewal, K.; Gadisa, A.; Oosterbaan, W. D.; Bertho, S.; Banishoeib, F.; Severen, I. V.; Lutsen, L.; Cleij, T. J.; Vanderzande, D.; Manca, J. V. *Adv. Funct. Mater.* **2008**, *18*, 2064–2070.
- (15) Scharber, M. C.; Mühlbacher, D.; Koppe, M.; Denk, P.; Waldauf, C.; Heeger, A. J.; Brabec, C. J. *Adv. Mater.* **2006**, *18*, 789–794.
- (16) Vandewal, K.; Tvingstedt, K.; Gadisa, A.; Inganäs, O.; Manca, J. V. *Phys. Rev. B* **2010**, *81*, 125204.
- (17) Tvingstedt, K.; Vandewal, K.; Gadisa, A.; Zhang, F.; Manca, J.; Inganäs, O. *J. Am. Chem. Soc.* **2009**, *131*, 11819–11824.
- (18) Markvart, T. *Appl. Phys. Lett.* **2007**, *91*, 064102.
- (19) Shuttle, C. G.; Hamilton, R.; O'Regan, B. C.; Nelson, J.; Durrant, J. R. *Proc. Natl. Acad. Sci. U.S.A.* **2010**, *107*, 16448–16452.
- (20) Maurano, A.; Hamilton, R.; Shuttle, C. G.; Ballantyne, A. M.; Nelson, J.; O'Regan, B.; Zhang, W.; McCulloch, I.; Azimi, H.; Morana, M.; Brabec, C. J.; Durrant, J. R. *Adv. Mater.* **2010**, *22*, 4987–4992.
- (21) Deibel, C.; Strobel, T.; Dyakonov, V. *Adv. Mater.* **2010**, *22*, 4097–4111.
- (22) Loi, M. A.; Toffanin, S.; Muccini, M.; Forster, M.; Scherf, U.; Scharber, M. *Adv. Funct. Mater.* **2007**, *17*, 2111–2116.
- (23) Benson-Smith, J. J.; Goris, L.; Vandewal, K.; Haenen, K.; Manca, J. V.; Vanderzande, D.; Bradley, D. D. C.; Nelson, J. *Adv. Funct. Mater.* **2007**, *17*, 451–457.
- (24) Westenhoff, S.; Howard, I. A.; Hodgkiss, J. M.; Kirov, K. R.; Bronstein, H. A.; Williams, C. K.; Greenham, N. C.; Friend, R. H. J. *Am. Chem. Soc.* **2008**, *130*, 13653–13658.
- (25) Dyer-Smith, C.; Reynolds, L. X.; Bruno, A.; Bradley, D. D. C.; Haque, S. A.; Nelson, J. *Adv. Funct. Mater.* **2010**, *20*, 2701–2708.
- (26) Benson-Smith, J. J.; Ohkita, H.; Cook, S.; Durrant, J. R.; Bradley, D. D. C.; Nelson, J. *Dalton Trans.* **2009**, 10000.
- (27) Ohkita, H.; Cook, S.; Astuti, Y.; Duffy, W.; Tierney, S.; Zhang, W.; Heeney, M.; McCulloch, I.; Nelson, J.; Bradley, D. D. C.; Durrant, J. R. *J. Am. Chem. Soc.* **2008**, *130*, 3030–3042.
- (28) Ishwara, T.; Bradley, D. D. C.; Nelson, J.; Ravirajan, P.; Vanseveren, I.; Cleij, T.; Vanderzande, D.; Lutsen, L.; Tierney, S.; Heeney, M.; McCulloch, I. *Appl. Phys. Lett.* **2008**, *92*, 053308.
- (29) Rand, B. P.; Burk, D. P.; Forrest, S. R. *Phys. Rev. B* **2007**, *75*, 115327.
- (30) Kim, Y.; Choulis, S. A.; Nelson, J.; Bradley, D. D. C.; Cook, S.; Durrant, J. R. *J. Mater. Sci.* **2005**, *40*, 1371–1376.
- (31) Andersson, L. M.; Inganäs, O. *Appl. Phys. Lett.* **2006**, *88*, 082103.
- (32) Kanai, K.; Akaike, K.; Koyasu, K.; Sakai, K.; Nishi, T.; Kamizuru, Y.; Nishi, T.; Ouchi, Y.; Seki, K. *Appl. Phys., A* **2009**, *95*, 309–313.
- (33) Guan, Z.-L.; Kim, J. B.; Wang, H.; Jaye, C.; Fischer, D. A.; Loo, Y.-L.; Kahn, A. *Org. Electron.* **2010**, *11*, 1779–1785.
- (34) Piersimoni, F.; Chambon, S.; Vandewal, K.; Mens, R.; Boonen, T.; Gadisa, A.; Izquierdo, M.; Filippone, S.; Ruttens, B.; D'Haen, J.; Martin, N.; Lutsen, L.; Vanderzande, D.; Adriaenssens, P.; Manca, J. V. *J. Phys. Chem. C* **2011**, *115*, 10873–10880.
- (35) Koch, N. *ChemPhysChem* **2007**, *8*, 1438–1455.
- (36) Tsoi, W. C.; Spencer, S. J.; Yang, L.; Ballantyne, A. M.; Nicholson, P. G.; Turnbull, A.; Shard, A. G.; Murphy, C. E.; Bradley, D. D. C.; Nelson, J.; Kim, J.-S. *Macromolecules* **2011**, *44*, 2944–2952.
- (37) Aarnio, H.; Sehati, P.; Braun, S.; Nyman, M.; de Jong, M. P.; Fahlman, M.; Österbacka, R. *Adv. Energy Mater.* **2011**, *1*, 792–797.
- (38) Frost, J. M.; Faist, M. A.; Nelson, J. *Adv. Mater.* **2010**, *22*, 4881–4884.
- (39) Slooff, L. H.; Veenstra, S. C.; Kroon, J. M.; Moet, D. J. D.; Sweelssen, J.; Koetse, M. M. *Appl. Phys. Lett.* **2007**, *90*, 143506.
- (40) Veldman, D.; Ipek, Ö.; Meskers, S. C. J.; Sweelssen, J.; Koetse, M. M.; Veenstra, S. C.; Kroon, J. M.; Bavel, S. S.; van; Loos, J.; Janssen, R. A. J. *J. Am. Chem. Soc.* **2008**, *130*, 7721–7735.
- (41) Inganäs, O.; Svensson, M.; Gadisa, A.; Zhang, F.; Persson, N. K.; Wang, X.; Andersson, M. R. *Appl. Phys., A* **2004**, *79*, 31–35.
- (42) Vandewal, K.; Tvingstedt, K.; Gadisa, A.; Inganäs, O.; Manca, J. V. *Nat. Mater.* **2009**, *8*, 904–909.
- (43) He, Y.; Chen, H.-Y.; Hou, J.; Li, Y. *J. Am. Chem. Soc.* **2010**, *132*, 1377–1382.
- (44) Ma, W.; Yang, C.; Gong, X.; Lee, K.; Heeger, A. J. *Adv. Funct. Mater.* **2005**, *15*, 1617–1622.
- (45) Li, G.; Shrotriya, V.; Huang, J.; Yao, Y.; Moriarty, T.; Emery, K.; Yang, Y. *Nat. Mater.* **2005**, *4*, 864–868.
- (46) Li, G.; Yao, Y.; Yang, H.; Shrotriya, V.; Yang, G.; Yang, Y. *Adv. Funct. Mater.* **2007**, *17*, 1636–1644.
- (47) Campoy-Quiles, M.; Ferenczi, T.; Agostinelli, T.; Etchegoin, P. G.; Kim, Y.; Anthopoulos, T. D.; Stavrinou, P. N.; Bradley, D. D. C.; Nelson, J. *Nat. Mater.* **2008**, *7*, 158–164.
- (48) Veenstra, S. C.; Verhees, W. J. H.; Kroon, J. M.; Koetse, M. M.; Sweelssen, J.; Bastiaansen, J. J. A. M.; Schoo, H. F. M.; Yang, X.; Alexeev, A.; Loos, J.; Schubert, U. S.; Wienk, M. M. *Chem. Mater.* **2011**, *16*, 2503–2508.
- (49) Irwin, M. D.; Buchholz, D. B.; Hains, A. W.; Chang, R. P. H.; Marks, T. J. *Proc. Natl. Acad. Sci. U.S.A.* **2008**, *105*, 2783–2787.
- (50) Hou, J.; Chen, H.-Y.; Zhang, S.; Li, G.; Yang, Y. *J. Am. Chem. Soc.* **2008**, *130*, 16144–16145.
- (51) Morteani, A. C.; Dhoot, A. S.; Kim, J.-S.; Silva, C.; Greenham, N. C.; Murphy, C.; Moons, E.; Ciná, S.; Burroughes, J. H.; Friend, R. H. *Adv. Mater.* **2003**, *15*, 1708–1712.
- (52) Morteani, A. C.; Ho, P. K. H.; Friend, R. H.; Silva, C. *Appl. Phys. Lett.* **2005**, *86*, 163501.
- (53) Morteani, A. C.; Sreearunothai, P.; Herz, L. M.; Friend, R. H.; Silva, C. *Phys. Rev. Lett.* **2004**, *92*, 247402.
- (54) Hertel, D.; Bäessler, H. *ChemPhysChem* **2008**, *9*, 666–688.
- (55) Frost, J. M.; Faist, M. A.; Nelson, J. *Adv. Mater.* **2010**, *22*, 4881–4884.

(56) Soon, Y. W.; Clarke, T. M.; Zhang, W.; Agostinelli, T.; Kirkpatrick, J.; Dyer-Smith, C.; McCulloch, I.; Nelson, J.; Durrant, J. R. *Chem. Sci.* **2011**, *2*, 1111–1120.

(57) Clarke, T.; Ballantyne, A.; Jamieson, F.; Brabec, C.; Nelson, J.; Durrant, J. *Chem. Commun.* **2009**, 89.

(58) Dean, P. J.; Haynes, J. R.; Flood, W. F. *Phys. Rev.* **1967**, *161*, 711.

(59) Ballantyne, A. M.; Chen, L.; Dane, J.; Hammant, T.; Braun, F. M.; Heeney, M.; Duffy, W.; McCulloch, I.; Bradley, D. D. C.; Nelson, J. *Adv. Funct. Mater.* **2008**, *18*, 2373–2380.

(60) Rau, U. *Phys. Rev. B* **2007**, *76*, 085303.

(61) Kirchartz, T.; Rau, U. *Phys. Status Solidi A* **2008**, *205*, 2737–2751.

(62) Hoyer, U.; Pinna, L.; Swonke, T.; Auer, R.; Brabec, C. J.; Stubhan, T.; Li, N. *Adv. Energy Mater.* **2011**, *1*, 1097–1100.

(63) Kirchartz, T.; Rau, U. *J. Appl. Phys.* **2007**, *102*, 104510.

(64) Kirchartz, T.; Rau, U.; Kurth, M.; Mattheis, J.; Werner, J. *Thin Solid Films* **2007**, *515*, 6238–6242.

(65) Kirchartz, T.; Pieters, B. E.; Kirkpatrick, J.; Rau, U.; Nelson, J. *Phys. Rev. B* **2011**, *83*, 115209.

(66) Liang, Z.; Reese, M. O.; Gregg, B. A. *ACS Appl. Mater. Interfaces* **2011**, *3*, 2042–2050.

(67) Street, R. A.; Song, K. W.; Northrup, J. E.; Cowan, S. *Phys. Rev. B* **2011**, *83*, 165207.

(68) Street, R. A. *Phys. Rev. B* **2011**, *84*, 075208.

(69) Ooi, Z. E.; Tam, T. L.; Shin, R. Y. C.; Chen, Z. K.; Kietzke, T.; Sellinger, A.; Baumgarten, M.; Mullen, K.; deMello, J. C. *J. Mater. Chem.* **2008**, *18*, 4619–4622.

(70) Koetse, M. M.; Sweelssen, J.; Hoekerd, K. T.; Schoo, H. F. M.; Veenstra, S. C.; Kroon, J. M.; Yang, X.; Loos, J. *Appl. Phys. Lett.* **2006**, *88*, 083504–3.

(71) Brunetti, F. G.; Gong, X.; Tong, M.; Heeger, A. J.; Wudl, F. *Angew. Chem., Int. Ed.* **2010**, *49*, 532–536.

(72) Hörmann, U.; Wagner, J.; Gruber, M.; Opitz, A.; Brütting, W. *physica status solidi (RRL) - Rapid Research Letters* **2011**, *5*, 241–243.

(73) Dennler, G.; Scharber, M. C.; Ameri, T.; Denk, P.; Forberich, K.; Waldauf, C.; Brabec, C. J. *Adv. Mater.* **2008**, *20*, 579–583.

(74) Bijleveld, J. C.; Zoombelt, A. P.; Mathijssen, S. G. J.; Wienk, M. M.; Turbiez, M.; de Leeuw, D. M.; Janssen, R. A. J. *J. Am. Chem. Soc.* **2009**, *131*, 16616–16617.

(75) Green, M. A.; Emery, K.; Hishikawa, Y.; Warta, W. *Progress in Photovoltaics: Research and Applications* **2011**, *19*, 84–92.

(76) He, Z.; Zhong, C.; Huang, X.; Wong, W.; Wu, H.; Chen, L.; Su, S.; Cao, Y. *Adv. Mater.* **2011**, *23*, 4636–4643.